by increasing the number of the phases for a constant clock frequency and signal bandwidth. It can also be noted that for practical reasons the ratio $f_c/(2f_0)$ should be chosen greater than 32.

For a given application, the optimal values of N and $f_c/(2f_0)$ can be selected using eqn. 3 or from Fig. 2. It should be noted that the SNR values shown in Fig. 2 can be improved by an additional 9·5, 16·9, 23·5 or 29·8 dB, if 2, 3, 4 or 5 bit internal quantisers are used, respectively.

Simulation results: Extensive simulations were performed to verify the improved system performance of the multiplexed noise-shaping structures. In Fig. 3 the power spectral densities of the system in Fig. 1 with 1 bit DAC, ideal 5 bit ADC and DAC, and nonideal 5 bit ADC and DAC with an RMS non-linearity equal to 0·1 LSB are plotted. We note that 5 bit quantisers are used only during period $\phi_3 = 1$. Fig. 3 demonstrates a further increase in resolution by employing multibit quantisers during the last phase ($\phi_N = 1$). The degradation due to the DAC nonlinearity is small because nonlinearity noise is also highpass filtered by a second-order noise-shaping function.
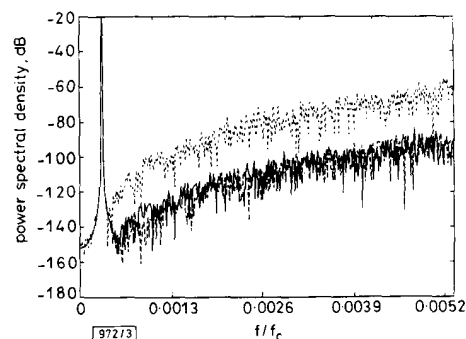

Fig. 3 *Power spectrum of system in Fig. 1 with single- and multibit quantisers*

------- 1 bit ADC/DAC
– – – – Ideal 5 bit ADC/DAC
———— 0·1 LSB nonlinear 5 bit ADC/DAC

Fig. 4 compares the signal-to-noise plus distortion (S/N + D) performances of a 3 phase multiplexed modulator with various quantisers; 1 bit, ideal 5 bit and 0·1 LSB RMS nonlinear 5 bit ADC and DAC. As explained before, the multibit quantiser is only employed in the last phase. It should be noted that the above SNR results were obtained for the ratio $f_c/(2f_0) = 96$.
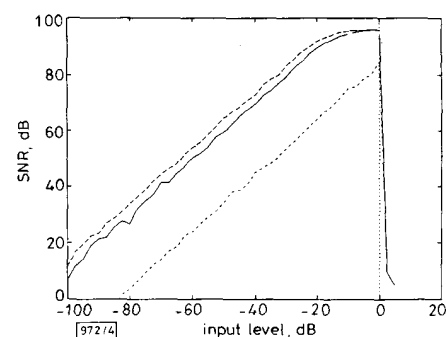

Fig. 4 *SNR against input level for proposed system in Fig. 1 with* $f_c/(2f_0) = 96$

------- 1 bit ADC/DAC
– – – – Ideal 5 bit ADC/DAC
———— 0·1 LSB nonlinear 5 bit ADC/DAC

Conclusions: A multiplexed $\Delta\Sigma$ A/D structure was proposed. It was shown that high-resolution conversion can be economically achieved under practical conditions. The above concept can be easily applied to higher-order (second-, or even third-order) $\Delta\Sigma$ modulators. It seems also promising for bandpass $\Delta\Sigma$ A/D applications. However, it was also observed that the gain of an additional feedback path is a critical parameter in the overall system performance. This problem will be addressed in future publications.

Z. CZARNUL*   *4th October 1991*
A. G. YESILYURT
G. C. TEMES
Oregon State University
Department of Electrical and Computer Eng.
Corvallis, Oregon

* On leave from the Institute of Electronic Technology, Technical University of Gdansk, Poland

References

1 CANDY, J. C., and TEMES, G. C. (Eds.): 'Oversampling delta–sigma data convertors' (IEEE Press, New York, 1991)
2 LESLIE, T. C., and SINGH, B.: 'An improved sigma–delta architecture'. Proc. IEEE Int. Symp. Circuits and Systems, 1990, pp. 372–375
3 BRANDT, B. P., and WOOLEY, B. A.: 'A CMOS oversampling A/D converter with 12b resolution at conversion rates above 1 MHz'. Dig. IEEE Int. Solid-State Circuits Conf., 1991, pp. 64–65
4 LARSON, L. E., CATALTEPE, T., and TEMES, G. C.: 'Multibit over-sampled $\Delta\Sigma$ A/D convertor with digital error correction', *Electron. Lett.*, 1988, **24**, pp. 1051–1052
5 HAIRAPETIAN, A., TEMES, G. C., and ZHANG, Z. X.: 'Multibit sigma–delta modulator with reduced sensitivity to DAC nonlinearity', *Electron. Lett.*, 1991, **27**, pp. 990–991
6 CZARNUL, Z., TEMES, G. C., and YESILYURT, A. G.: 'Pseudo-N-path switched capacitor filters with out-of-band noise peaks', *Electron. Lett.*, 1991, **27**, pp. 1137–1139

COMPARISON OF DIFFERENTIAL GAIN IN SINGLE QUANTUM WELL AND BULK DOUBLE HETEROSTRUCTURE LASERS

Indexing terms: Semiconductor lasers, Lasers

The differential gain in single quantum well and bulk double heterostructure lasers is compared. In variance with previous predictions, no differential gain enhancement is found in single quantum well structure lasers at room temperature. Only at low temperatures do the quantum well lasers possess higher differential gain than bulk double heterostructure lasers. The results have important implications in the area of high speed phenomena for these devices.

The most important material parameter, which determines the pulse response and modulation bandwidth of semiconductor lasers, is the differential gain, which is the derivative of the bulk gain with respect to the carrier density. The differential gain and the resonance frequency, usually taken as the upper modulation limit, are related by[1]

$$f_r = \frac{1}{2\pi}\sqrt{\left(\frac{v_g P_0 G_0'}{\tau_p}\right)} \tag{1}$$

where v_g is the photon group velocity, P_0 is the photon density at the active region, τ_p is the photon lifetime, $G_0' = dG_0/dN$ is the (linear) differential gain. G_0 and N are the linear gain constant and the carrier density, respectively. Eqn. 1 suggests that increasing the photon density P_0 increases the

modulation bandwidth. This strategy is defeated eventually by the nonlinear gain phenomenon[2] and it can be shown that the maximum 0 dB rolloff modulation frequency is

$$f_{0\,dB}^{max} = \frac{1}{2\pi} \frac{v_g G_0 G_0'}{\dfrac{G_0'}{\Gamma_c} + \dfrac{G_1}{P_s}}$$ (2)

where G_1 is the nonlinear gain constant, P_s is the saturation photon density and Γ_c is the confinement factor which depends on the laser structure and the injected carrier dimensionality. Details of the derivation of eqn. 2 will be discussed elsewhere. These results indicate that the differential gain is directly related to the intrinsic modulation bandwidth. Higher differential gain will lead to larger modulation bandwidth.

Quantum well (QW) lasers have been previously predicted to have enhanced differential gain compared to conventional bulk double heterostructure (DH) lasers.[3–5] This differential gain enhancement was attributed to the abrupt step-like two-dimensional (2-D) density of states in QW lasers. We present the results of a theoretical comparison of the differential gain in 2-D single QW lasers and bulk DH lasers. We find that there is no differential gain enhancement in the single QW lasers compared to the DH lasers at room temperature. The single QW lasers possess a higher differential gain than the DH lasers only at low temepratures. At high temperatures, including room temperature, the effects of the Fermi occupation statistics and the step-like 2-D density of states in the QW structures lead to a lower differential gain.

The linear optical gain with photon energy E derived under a k-selection rule is given by

$$G_0(E) = B \frac{E}{n_r} \sum_{i=l,\,h} \int \delta_i \rho_i(\xi)(f_e + f_h - 1)$$

$$\times \frac{\hbar/T_2}{(\xi - E)^2 + (\hbar/T_2)^2}\, d\xi$$ (3)

where B is a constant, n_r is the modal effective refractive index, f_e and f_h are the quasi-Fermi distribution functions for electrons and holes respectively, ρ_i is either the step-like 2-D reduced density of states for the QW structure or the parabolic three-dimensional (3-D) reduced density of states for the DH structure, i designates either light holes ($i = l$) or heavy holes ($i = h$) and δ_i is the polarisation modification factor for the dipole moment.[6] The injected carrier density N in the QW structure and the DH structure are computed by integrating the products of corresponding density of states and quasi-Fermi functions.

We compare the differential gain G_0' at the gain peak of QW lasers and DH lasers in the well known GaAs/AlGaAs material system. A typical QW laser structure with symmetric 4000 Å $Al_{0.5}Ga_{0.5}As/Al_{0.2}Ga_{0.8}As$ graded index separate confinement heterostructure (GRINSCH) and a 100 Å quantum well located at its centre is assumed. For the DH lasers we assume a typical $Al_{0.35}Ga_{0.65}As/GaAs$ DH with GaAs active layer thickness 0.1 μm. Effective masses $m_e = 0.067m_0$, $m_{hh} = 0.45m_0$ and $m_{lh} = 0.082m_0$ are used for electrons, heavy holes and light holes, respectively. The gain is calculated for TE mode and the collisional broadening time $T_2 = 0.1$ ps is used. It is essential that in calculating the injected carrier density in the QW structure we account for the population of carriers in the GRIN optical confining region.

In Fig. 1 we show the differential gain of the QW structure and of the DH structure as a function of the modal gain $(g_{modal} = \Gamma_c G_0)$ at room temperature ($T = 300$ K). The transverse effective optical mode width is evaluated as 0.281 μm for the QW structure and 0.305 μm for the DH structure, respectively. The effective optical mode widths are used to obtain the corresponding confinement factors Γ_c. Fig. 1 shows that there is no differential gain enhancement in the QW structure at room temperature. The differential gain of the QW structure is comparable with that of the DH structure in the very low modal gain region. In the large modal gain region, the DH structure possesses higher differential gain. The decrease in G_0' with increasing modal gain in the QW structure results

from the finite available gain per quantised state. The abrupt increase $(g_{modal} \simeq 80\,cm^{-1})$ in G_0' in the QW structure is due to the onset of the second quantised states of the QW.
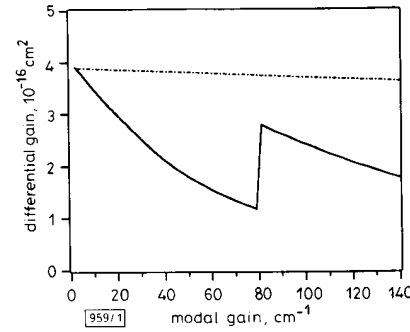

Fig. 1 *Differential gain of assumed single QW and assumed DH lasers as functions of modal gain at room temperature $T = 300$ K*

— · — · DH structure
———— QW structure

Fig. 2 shows the computed differential gain of the QW structure and of the DH structure as a function of the modal gain at $T = 77$ K. The differential gain is seen to be enhanced in the QW structure at this low temperature. The differential gain enhancement relative to the DH structure is as high as ~300% at low modal gain. In Fig. 3, we show the differential gain of the QW structure and the DH structure lasers as functions of modal gain at high temperature $T = 400$ K. The DH structure has higher differential gain over all the modal gain region at this high temperature.
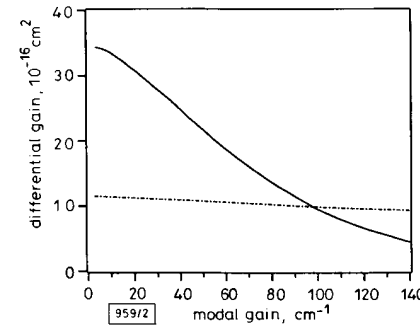

Fig. 2 *Differential gain of assumed single QW and assumed DH lasers as functions of modal gain at low temperature $T = 77$ K*

— · — · DH structure
———— QW structure

Figs. 1–3 indicate the differential gain is increased in both the QW structure and the DH structure as the temperature is decreased. The increase of the differential gain with decreasing of temperature is due to the more abrupt transition region of the Fermi–Dirac occupation function for electrons (and holes) at lower temperatures which increases the density of electrons (and holes), at given total injected electron (and hole) density, near the optical transition energy. Figs. 1–3 also show that the differential gain of the QW lasers changes more rapidly with the temperature change compared to the DH lasers. The result is that the modulation dynamics in the QW lasers is more strongly affected by the temperature. The thermal dissipation is more important in the QW structure lasers for high speed performance.

The qualitative physical reason for the predicted reduced differential gain of the single QW lasers relative to the DH lasers at room temperature or higher temperatures is as follows. An increasing fraction of the injected carriers at room temperature goes into occupation of the large density of states in the GRIN confining region. These electrons (and holes) contribute little to the gain because of the $(\varepsilon - E)^2$ term in the

ELECTRONICS LETTERS 5th December 1991 Vol. 27 No. 25

denominator of eqn. 3. On the other hand, the optical gain is limited due to the flat feature of the 2-D step-like density of states for the QW structure. The result is a lowering of $G_0' = dG_0/dN$ in the QW structure. At lower temperatures however, the Fermi–Dirac occupation factor for these GRIN states is reduced considerably. In addition, the more abrupt cutoff of the Fermi–Dirac occupation functions at low temperatures take advantage of the step-like 2-D density of states profile in contributing to relatively large increase in G_0 with increasing N.
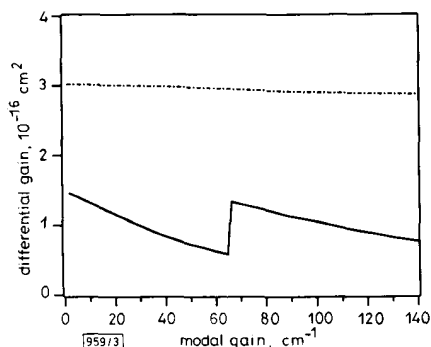

Fig. 3 *Differential gain of assumed single QW and assumed DH lasers as functions of modal gain at high temperature $T = 400\,K$*
— · — · DH structure
——— QW structure

In summary, we find that there is no differential gain enhancement in single QW structure lasers compared to DH lasers at room temperature. The QW structure lasers possess enhanced differential gain compared to the DH lasers only at low temperatures. The modulation dynamics in the QW structure is more strongly affected by the temperature.

B. ZHAO   2nd October 1991
T. R. CHEN
A. YARIV

T. J. Watson Sr. Laboratories of Applied Physics, 128-95
California Institute of Technology
Pasadena, California 91125, USA

References

1 LAU, K. Y., BAR-CHAIM, N., URY, I., HARDER, CH., and YARIV, A.: 'Direct amplitude modulation of short-cavity GaAs lasers up to X-band frequencies', *Appl. Phys. Lett.*, 1983, **43**, pp. 1–3

2 YAMADA, M., and SUEMATSU, Y.: 'Analysis of gain suppression in undoped injection lasers', *J. Appl. Phys.*, 1981m **52**, pp. 2653–2664

3 BURT, M. G.: 'Gain spectra of quantum-well lasers', *Electron. Lett.*, 1983, **19**, pp. 210–211

4 ARAKAWA, Y., VAHALA, K., and YARIV, A.: 'Quantum noise and dynamics in quantum well and quantum wire lasers', *Appl. Phys. Lett.*, 1984, **45**, pp. 950–952

5 ARAKAWA, Y., and YARIV, A.: 'Quantum well lasers—gain, spectra, dynamics', *IEEE J. Quantum Electron.*, 1986, **QE-22**, pp. 1887–1899

6 YAMADA, M., OGITA, S., YAMAGISHI, M., TABATA, K., NAKAYA, N., ASADA, M., and SUEMATSU, Y.: 'Polarization-dependent gain in GaAs/AlGaAs multiquantum-well lasers: theory and experiment', *Appl. Phys. Lett.*, 1984, **45**, pp. 324–325

MINIMISATION OF REFLECTION COEFFICIENT AT FEED OF RADOME-COVERED REFLECTOR ANTENNA BY CHIRAL DEVICE

Indexing terms: Antennas, Reflector antennas

A method is proposed which consists of placing a chiral device in the central region of a radome covering a reflector antenna, to minimise the reflection coefficient at the antenna feed and any possible distortion in the antenna radiation pattern due to the device.

The reflection coefficient at the feed of a radome-covered reflector antenna has been studied.[1-4] It has been found that it is the central region of the radome which contributes most to its value. A method for reducing the return loss by placing a hemispherical iris-loaded sandwich section in this region has been investigated.[3-4] Typically, a 5 dB reduction in antenna return loss can be achieved in the neighbourhood of a design frequency of 6·2 GHz in this way. An alternative possible method, which consists in placing a chiral device in the central region of the radome, is proposed in this Letter.

A three-dimensional chiral object is an object which cannot be brought into congruence with its mirror image by translation or rotation, so that a collection of chiral objects embedded in a host material forms a composite medium which is characterised by a right or left handedness. A linearly polarised wave propagating in a chiral medium is split into two waves, right and left-circularly polarised, which have different phase velocities. Thorough reviews on chiral media have appeared in the literature in recent years.[5-7] The radiation of a short electric dipole situated at the centre of a chiral sphere has been studied[8,9] and results of these studies indicate the potential use of chiral materials for making antenna radomes. Electromagnetic wave propagation through chiral slabs has been studied for analysing experimental data obtained in the remote sensing of vegetation layers[10] and for shielding applications through control of absorption and reflection.[11] It is interesting to examine the frequency behaviour of the reflectance and the transmittance of an electromagnetic wave propagating through a chiral slab which is designed to meet some predetermined requirements and placed in the central region of a radome.

It has been shown[1-4] that the absolute value of the reflection coefficient at the feed of a paraboloidal reflector antenna covered with a paraboloidal radome is given by

$$|\Gamma| = \left| \frac{G_0 \exp(-2jk_0 f)}{2k_0 f} \right.$$
$$\left. \times \left[1 + \frac{f'}{f} R \exp\{-2jk_0(f+f'-d)\} \right] \right| \quad (1)$$

where G_0 is the value at boresight of the circularly symmetric Gaussian gain of the linearly polarised point-source feed. f and f' are the reflector and radome focal distances, respectively, and d is the distance between the foci. R is the reflection coefficient at the boresight of the radome. We see that the reflection coefficient at the feed due to the reflector alone, i.e. $|(G_0/2k_0 f) \exp(-2jk_0 f)|$ is modulated by an expression containing R. Our purpose is to minimise the reflectance $|R|^2$ and concurrently to maximise the copolar transmittance and to minimise the crosspolar one.

The reflectances and the transmittances of the chiral slab at normal incidence have been calculated and are given by

$$_\perp\rho_\perp = [r_{12}^2 + r_{23}^2 + 2r_{12}r_{23}\cos(h_R + h_L)d]\Delta^{-1} \quad (2)$$

$$_\perp\rho_\parallel = 0 \quad (3)$$

$$_\perp\tau_\perp = (n_3/n_1)[0\cdot5t_{12}^2 t_{23}^2\{1 + \cos(h_R - h_L)d\}]\Delta^{-1} \quad (4)$$

$$_\perp\tau_\parallel = (n_3/n_1)[0\cdot5t_{12}^2 t_{23}^2\{1 - \cos(h_R - h_L)d\}]\Delta^{-1} \quad (5)$$

where $\Delta = 1 + r_{12}^2 r_{23}^2 + 2r_{12}r_{23}\cos(h_R + h_L)d$. The right index in ρ and τ indicates that the incident wave electric field is perpendicular ($\perp$) or parallel ($\parallel$) to an (arbitrary) plane containing the wave normal and the left index indicates that the reflected (or transmitted) wave electric field is perpendicular ($\perp$) or parallel ($\parallel$) to this plane. The wave numbers h_R and h_L are given by $h_R = \omega\mu_2\gamma_2 + (\omega^2\mu_2^2\gamma_2^2 + k_2^2)^{1/2}$ and $h_L = -\omega\mu_2\gamma_2 + (\omega^2\mu_2^2\gamma_2^2 + k_2^2)^{1/2}$, where $k_2^2 = \omega^{2n^2}\varepsilon_2$ and ε_2, μ_2, γ_2 are the permittivity, permeability and chirality admittance of the chiral slab, respectively (medium 2). The interface reflection and transmission coefficients are given by $r_{ij} = (Z_j - Z_i)/(Z_j + Z_i)$ ($i, j = 1, 2, 3$) and $t_{ij} = (2Z_j)/(Z_j + Z_i)$ ($i, j = 1, 2, 3$), where $Z_m = [(\mu_m/\varepsilon_m)/\{1 + \gamma_m^2(\mu_m/\varepsilon_m)\}]^{1/2}$. The wave is reflected in medium 1 and transmitted in medium 3. It is easy to show that in the limit where $\gamma_m \to 0$, the above expressions tend to